



JOINT INSTITUTE FOR NUCLEAR RESEARCH

Frank Laboratory of Neutron Physics

FINAL REPORT ON THE START PROGRAMME

Investigation of pulse shape discrimination characteristics of EJ-309 liquid scintillators for the experiment to study prompt neutron emission in nuclear fission

Supervisor:

Dr. Gadir Ahmadov

Student:

Deniel Rodriguez Almora, Cuba

Universidad de La Habana

Participation period:

July 21 – August 30,

Summer Session 2024

Abstract

Understanding the fission process, especially how energy is shared between fission fragments, is crucial for both fundamental science and practical applications. Investigations into prompt fission neutron (PFN) emission offer a window into this complex process. Research conducted at the Joint Institute for Nuclear Research (JINR) has been at the forefront of this field for over two decades, investigating the correlation between fission fragment characteristic (such as mass and kinetic energy) and neutron energy. These studies have uncovered complex patterns in how these variables fluctuate, shedding light on the stochastic nature of the fission process. Notably, recent experiments measuring PFN multiplicity have yielded unexpected results, suggesting that our current understanding of neutron emission mechanisms may be incomplete.

These surprising findings have reignited scientific interest and underscored the necessity for more refined experimental investigations. As a result, advanced experimental setups are being developed to explore these phenomena. At the Frank Laboratory of Neutron Physics, the ENGREN facility, comprising 32 liquid scintillators and a fission chamber, is being constructed to facilitate these studies. This facility aims to provide high-resolution data on neutron and gamma-ray emissions, allowing for a more nuanced understanding of the fission process.

The present work focuses on rigorously testing various components of this experimental setup to ensure their optimal performance. This includes calibrating the scintillators for accurate neutron detection and refining techniques for distinguishing between neutrons and gamma rays. Achieving optimal discrimination is critical for minimizing background noise and enhancing the precision of measurements.

1. Introduction

The primary objective of this setup is to investigate potential correlations between variations in prompt fission neutron (PFN) multiplicity and the total kinetic energy (TKE) of fission fragments (FF). Over the past six decades, research into PFN properties has made significant advancements, partly due to the refinement of the low geometric efficiency (LGE) method initially proposed by [1]. Further innovations introduced the use of a twin back-to-back ionization chamber (TBIC) for studying correlated properties of fission fragments and PFN emissions [2].

Correction of PFN multiplicity dependence on FF mass and TKE for $^{235}\text{U}(\text{nth},\text{f})$ reaction was reported in [3]. Investigations carried out in IBR30 in 1999-2000 pulsed reactor in Dubna [4, 5], confirmed existence of TKE variations in neutron resonances first reported by F.-J. Hamsch et al in IRMM [6]. PFN multiplicity measurement with LGE was carried out at GELINA in 2007-2008, using PFN detectors from DEMON collaboration and TBIC loaded by 1 mg U^{235} . However, statistical accuracy of data taken in resonances was not enough for reliable PFN multiplicity analysis. Recently experiments, intended to investigate the correlations between FF TKE and PFN multiplicity variations was reported in [7, 8]. Authors used position-sensitive TBIC as FF detector and the array of 12 PFN detection modules. The aim of the experiment was simultaneous measurement of FF TKE and PFN multiplicity variation using LEM. However, simultaneous measurement of FF TKE and PFN has limitation on the target material weight (should be as thin as possible).

Therefore, it was developed setup with a chamber loaded by 230 mg ^{235}U target (99.999%) and PFN detector composed of 32 fast neutron detection modules (76 mm diameter, 51 mm thickness) located at distance ~ 54 cm from the target (LEM = 0.012). It is expected to improve the statistical accuracy of measurement at 9.2 flight path of IREN facility (full neutron beam intensity $\sim 2 \cdot 10^{11}$ sec/4 π) at least by order of magnitude. To ensure the reliability of the entire experimental process, it is imperative that each component operates under optimal conditions. This work is

this directed towards determining the appropriate operational voltage for each detector, thereby achieving optimal performance.

2. Experimental setup

A new setup was developed with a target positioned at the center a prompt fission neutron (PFN) detector array, which consists of 32 fast neutron detection modules. These modules are meticulously arranged on a spherical surface with a radius of approximately 54 cm from the target within the detection chamber, as illustrated in figure 1.

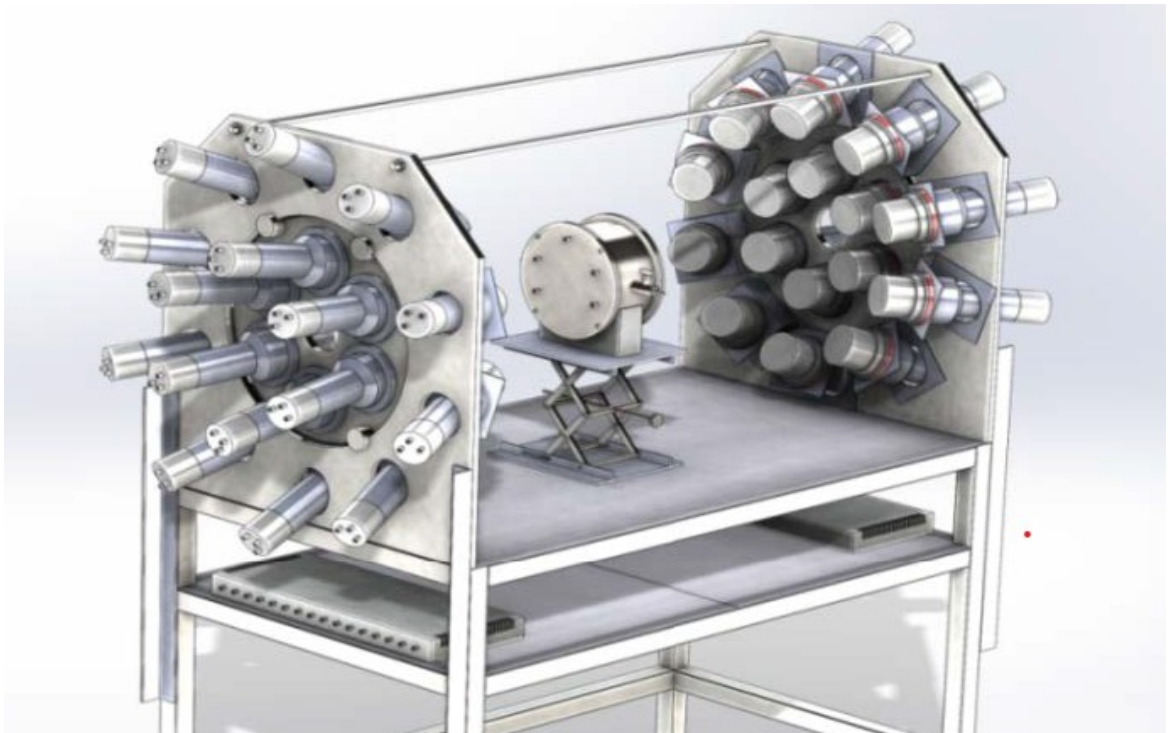


Figure 1. Drawing of the experimental setup

This configuration was specifically designed for the ENGREN project [9], to significantly enhance the statistical accuracy of neutron measurements along the 9.2-meter flight path of the IREN facility. The expected improvement in accuracy could be up to an order of magnitude. The enhanced precision of the measurements is due to the superior arrangement and high quality of the detection modules, coupled with the increased sensitivity resulting from the use of 32 modules, which collectively optimize neutron and gamma interaction detection. The spherical arrangement also offers an optimized detection geometry that facilitates comprehensive data collection.

2.1. Detectors

The project utilizes LS EJ-309 liquid scintillators, these radiation detectors were manufactured by Eljen Technology, Texas, USA. [10]. which are noted for their superior capability to distinguish between neutrons and gamma rays. The EJ-309 scintillator represents a significant improvement over traditional low-flash point PSD liquid scintillators that use xylene as a solvent. With a flash point of 144°C, the EJ-309 significantly reduces the fire hazards typically associated with low-flash point scintillators.

It offers several advantageous chemical properties that enhance its suitability for use in demanding environmental conditions. These properties include:

- **High Flash Point:** The elevated flash point of 144°C minimizes the risk of fire hazards, making the EJ-309 safer to handle and use.
- **Low Vapor Pressure:** The low vapor pressure reduces the risk of hazardous vapor release and contributes to a safer working environment.
- **Low Chemical Toxicity:** The reduced chemical toxicity of EJ-309 makes it a safer choice for laboratory and industrial applications.
- **Compatibility with Cast Acrylic Plastics:** The compatibility with cast acrylic plastics ensures that the scintillator can be effectively integrated into various detector designs without compatibility issues.

Figure 2 illustrates the emission spectrum of the EJ-309 scintillator, which peaks at a wavelength of 425 nm. This peak emission wavelength is indicative of the scintillator's efficiency in converting radiation into detectable light.

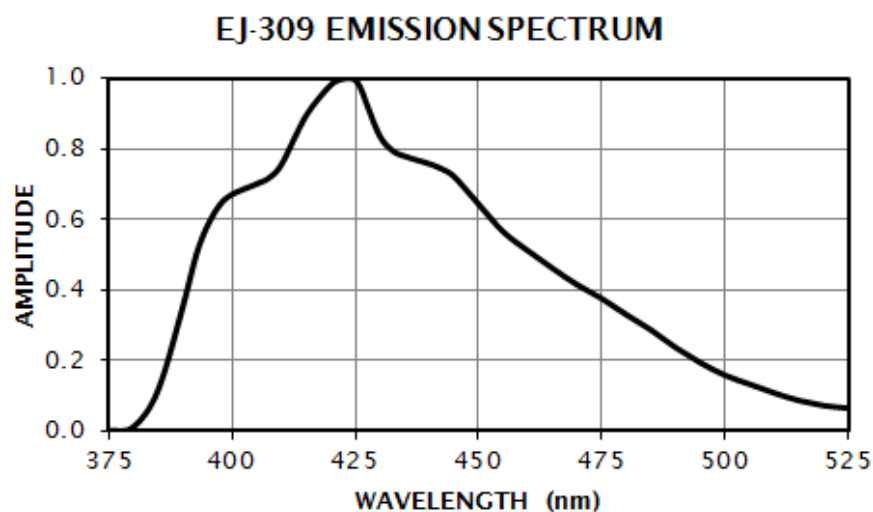


Figure 2. Emission Spectrum of LS EJ-309

Figure 2 provides an image of the EJ scintillation detector, which comprises an EJ scintillator coupled with a photomultiplier tube (PMT). Each detector has a diameter of 79.25 mm and a length of 77.30 mm as can be seen. In the figure 3. For (fast) neutron / gamma discrimination liquid scintillators in combination with pulse shape discriminating electronics are an effective solution, these liquid scintillators are hermetically sealed from ambient air. Liquid scintillators exhibit more thermal expansion than inorganic scintillators and every liquid scintillation cell needs an expansion reservoir, In order to allow at the same time neutron / gamma PSD and time-of-flight information, liquid scintillation detectors are usually equipped with fast (2-3 ns rise time) PMTs and transistorized, voltage dividers operated at negative high voltage [11].

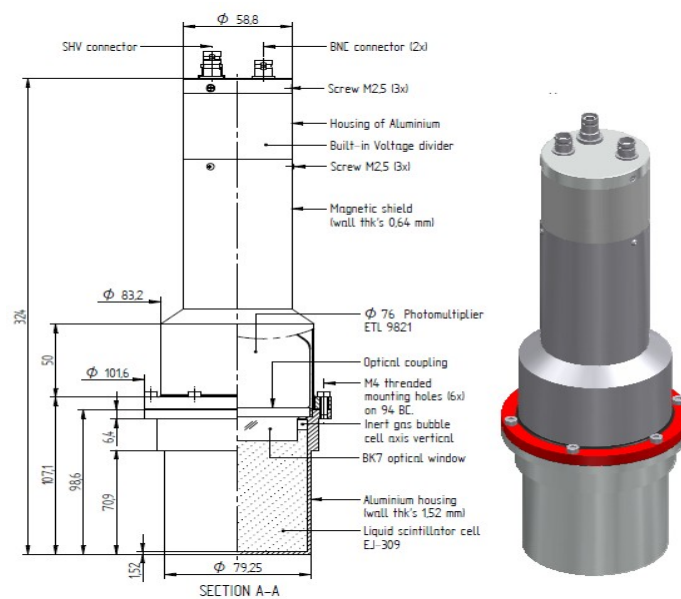


Figure 3. Representation of each of the components of the EJ-309 liquid scintillator

That is why the ETL 9821 photomultiplier is used in this detector, which is a 78 mm (3 in.) diameter end-window photomultiplier with a blue-green sensitive bialkali photocathode in a plano-concave window and 12 linearly focused BeCu dynodes for good linearity and timing [12].

2.2. Test of detectors

A critical step in the preparation of the experimental setup involved the determination of the operating voltage for each detector used to detect ionization radiation. Although the detectors were tested by the manufacturer prior to shipment, an additional verification of their operating voltages was performed.

While most detectors exhibited similar operating voltages, significant discrepancies were observed among a subset of detectors.

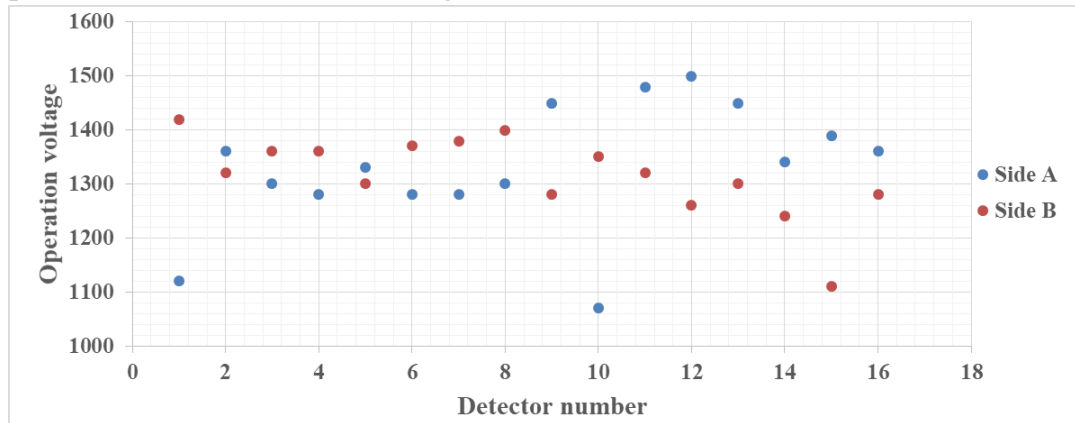


Figure 4. Dependence of operation voltage on detector number

^{60}Co source, positioned at the center of the setup (50 cm from the detector), was utilized to obtain consistent amplitude and count rate, with measurements facilitated by an oscilloscope. Following individual checks of each detector, a voltage divider with 16 outputs and one input was employed to bias the detectors. Two high-voltage power supplies were utilized to power all 32 detectors. The resistivity of the potentiometer was adjusted to allow for individual control of the voltage applied to the photomultiplier tubes (PMTs).

3. Measurement results

To evaluate the detectors and determine their actual efficiency, a comprehensive statistical analysis was performed using the ENGREN setup for event detection and ROOT software for statistical control and data evaluation. A series of point sources were used to ensure that each detector was registering and providing signals correctly. Initially, a ^{22}Na source was employed to conduct the necessary statistical analysis. Following this, a ^{60}Co source was introduced, and the same procedures were repeated to verify the consistency of the detectors' performance. After these tests, further measurements were performed using PuBe neutron source.

3.1. Measurement with gamma sources

After determining the optimal operating voltages for the detectors, measurements were conducted using two point calibration gamma sources. These sources were selected because they provide a range of known gamma-ray energies, which are essential for energy calibration and n/g discrimination in experiments conducted

within a mixed radiation field. Each source was positioned at a distance of 50 cm from the detectors, precisely at the center of the ENGREN setup. This is the designated location where the fission fragment (FF) detector is planned to be installed in future experiments. The placement was chosen to ensure consistent geometry and to replicate the conditions that will be used in the actual experimental setup, allowing for accurate calibration and preparation for subsequent data collection.

The Analog-to-Digital Converter (ADC) plays a crucial role in converting the analog signals generated by each detector into digital signals. This conversion facilitates the subsequent digital differentiation of each signal, enabling the identification of various particle types, such as distinguishing neutrons from gamma rays. In our setup, N6742 digitizer (switched capacitor digitizer based on the DRS4 chip) with 12-bit and adjustable sampling frequency from 0.75 to 5 GS/s was used for readout signals from detectors. Experimental block scheme of the detector-digitizer-PC connection shown on figure 5.



Figure 5. PMT – digitizer – PC connection

The generated signal from 16 PMTs is recorded CAEN N6742 Desktop Waveform Digitizer (16 Channel). Figure 6 presents waveform of recorded signal from one of the detectors.

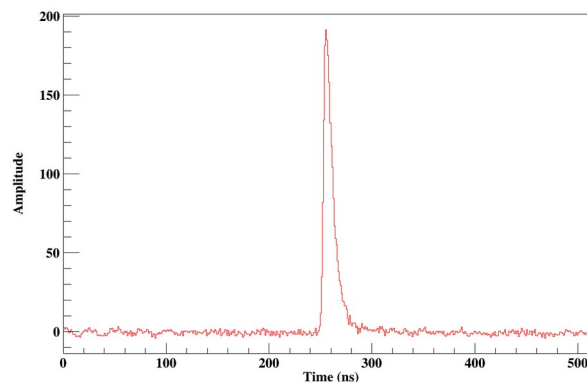


Figure 6. Recorded waveform from ^{60}Co gamma source for a single detector

Used CAEN digitizer let us to change sampling frequency from 750 MHz/s to 5 GHz/s and it is enough for fast signal registration. Data is taken in the self-triggering mode and recorded data are saved for offline analysis (figure 5) in a personal computer.

The digital signal processing serves as a tool for assessing the operational integrity of each detector by analyzing the recorded pulse heights. Variations in pulse height may indicate shifts in operational resistance or an incorrect trigger configuration. Figure 7 presents the pulse heights recorded by 16 detectors in response to ^{60}Co gamma-ray and PuBe neutron source. For the analysis of these pulse heights, ROOT-based scripts will be employed.

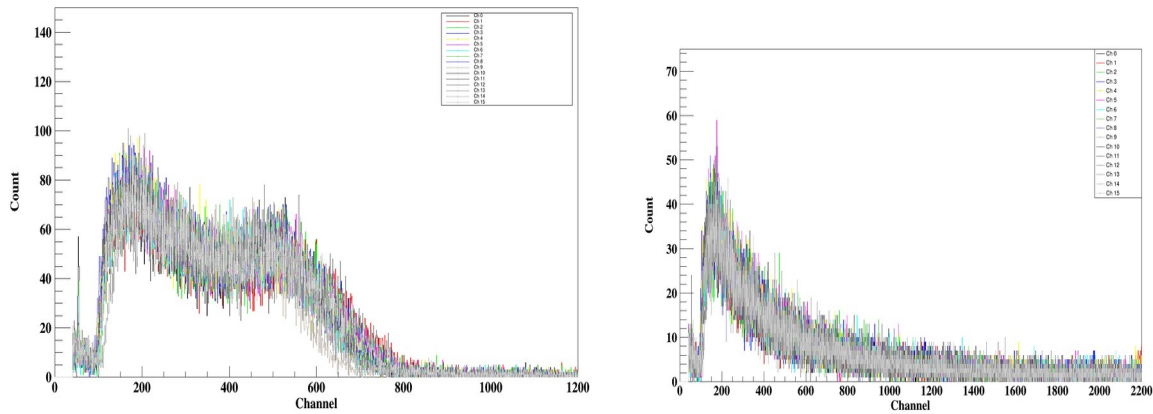


Figure 7. Pulse height spectrum of ^{60}Co gamma (left side) and PuBe neutron source (right side) from 16 detectors.

The pulse height spectra for all detectors are nearly identical, as shown in Figure 8, indicating that uniform gain was achieved across the detectors. To establish the relationship between the light output distribution and the actual energy deposited in the scintillator, as well as to define the thresholds, a gamma energy calibration was performed on the EJ-309 liquid scintillation detector using standard ^{22}Na and ^{60}Co gamma sources. Due to the material properties and interaction mechanisms of gamma rays in liquid scintillators, the resulting spectrum predominantly reflects electrons from Compton scattering. The position of the Compton edge was precisely determined by comparing the light output spectra from each source, as shown in figure 8. However, the peaks are not as well-defined as expected, likely due to the limited statistics collected, which can be attributed to the short exposure time of the detectors to each source. This is reflected in the spacing between the peaks.

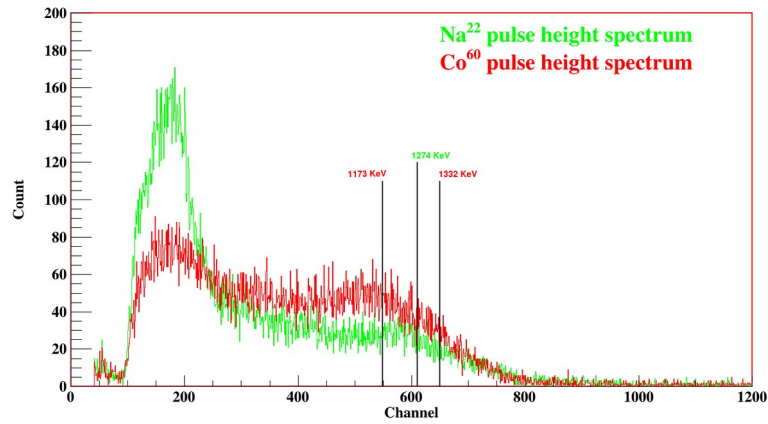


Figure 8. Gamma spectrum of the ^{60}Co and ^{22}Na gamma sources where the Compton edges of each spectrum can be seen.

3.3. Pulse shape discrimination method for gamma-rays and neutrons

There are two methods mainly used for discriminating between neutrons and gamma rays, which are planned to apply in our future experiments.

1. Pulse Shape Discrimination (PSD): PSD takes advantage of the distinct differences in the pulse shapes generated by neutrons and gamma rays when they interact with certain scintillating materials [13-14]. This technique analyzes the temporal profile of the light output, as neutrons typically produce pulses with a longer decay time compared to those generated by gamma rays. The difference in decay times allows for effective discrimination between the two types of radiation.
2. Time of Flight (TOF): The TOF method relies on the differing velocities of neutrons and gamma rays [15]. Gamma rays travel at the speed of light, while neutrons move significantly slower. By measuring the time it takes for each particle to travel from the source to the detector, it is possible to distinguish between neutrons and gamma rays based on their arrival times.

In this report, the results from the Pulse Shape Discrimination (PSD) method are presented. To determine the optimal neutron/gamma (n/γ) discrimination, experiments were conducted using a PuBe neutron source at various operating voltages. Figure 9 shows the pulse height spectra at different voltages. As illustrated in the figure, changing the operating voltage influences the gain of the photomultiplier tubes (PMTs), which can, in turn, affect the n/γ discrimination capability of the detectors.

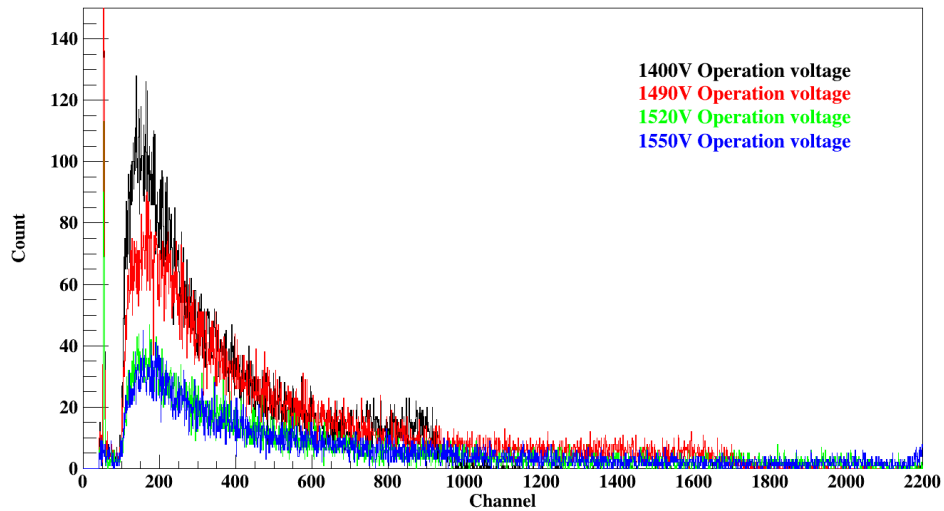


Figure 9. Pulse height distribution of a single detector exposed to a PuBe neutron source at varying operating voltages.

Figure 10 presents a two-dimensional scatter diagram illustrating n- γ discrimination via the charge comparison method. The plot reveals two distinct bands: the lower band correlates with neutrons, characterized by a larger slow discharge [16], while the upper band corresponds to gamma rays.

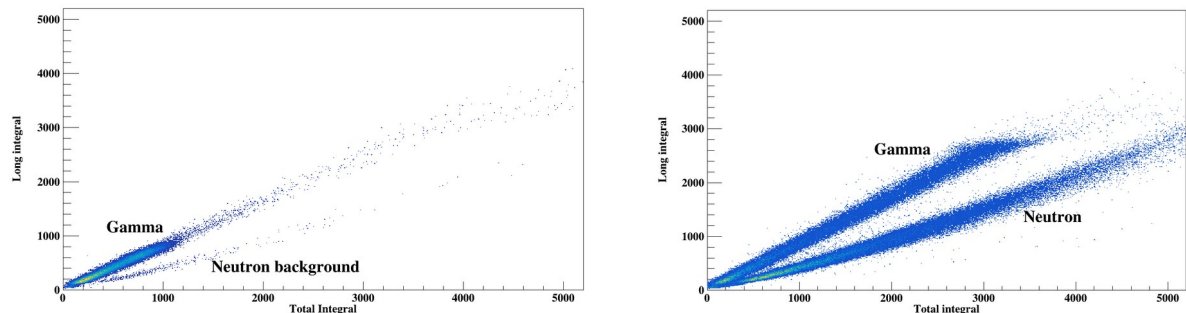


Figure 10. n- γ discrimination using the charge integration method for PuBe (right) and ^{60}Co (left)

Using a gamma source (Figure 10, left) instead of a neutron source (Figure 10, right) produced the expected result, with only background neutrons being detected. To evaluate the quality of neutron-gamma discrimination, peak values and average signal widths were analyzed, and the distance between the peaks was calculated to quantify this discrimination, yielding a value of 4.1. Figure 11 presents the ratio of the long-to-total integral (L/T) for ^{60}Co (black) and PuBe (red). The first peak corresponds to neutrons, while the second peak represents gamma rays.

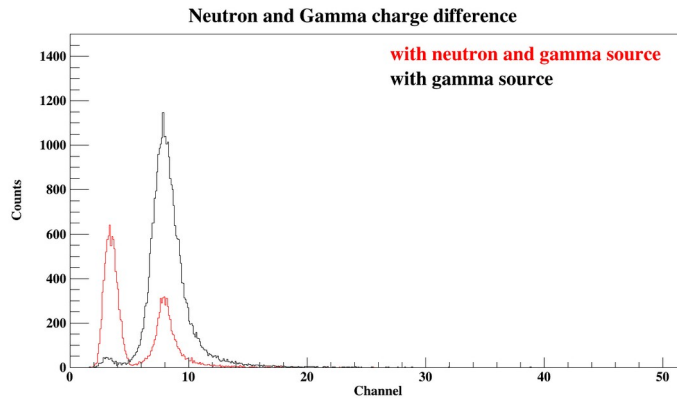


Figure 11. L/T integral for gamma and neutron sources

As shown, the gamma peaks from both ^{60}Co and PuBe align at the same position. Related peaks were fitted with a Gaussian function to precisely determine the peak centers. The distance between the gamma and neutron peaks was calculated, and the dependence of the distance between them on the operating voltage was shown in figure 12.

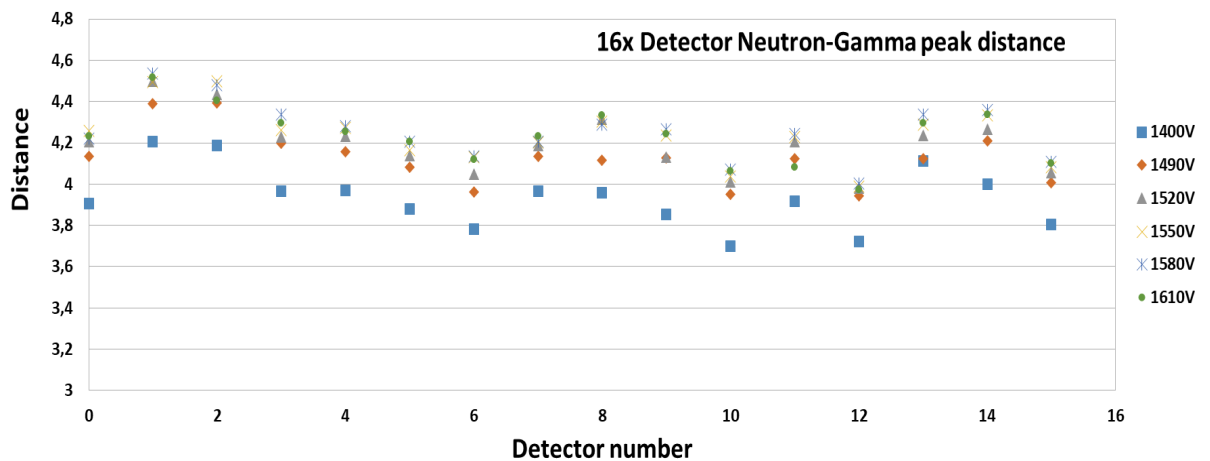


Figure 12. Dependence of distance between gamma and neutron peaks for every detector in different voltage.

As shown in the figure, the performance of neutron/gamma (n/ γ) discrimination varies with operating voltage. The optimal n/ γ discrimination performance was identified at specific operating voltages, and these optimal voltages were subsequently applied.

4. Conclusions

The EJ-309 liquid scintillators were tested using both gamma and neutron sources to determine their optimal operating voltages. Despite all 32 scintillators being of the same type, a variation of approximately 500 V in operating voltages was observed. Consequently, the ordered voltage divider was modified to allow for adjustments of up to 500 V to accommodate these differences.

The experiments on neutron/gamma (n/γ) discrimination demonstrated that the effectiveness of this discrimination is significantly affected by the operating voltage of the detectors. Analysis of the pulse height spectra revealed that while the gamma peaks from sources like ⁶⁰Co and PuBe align closely, careful optimization of operating voltages allows for distinct separation of neutron and gamma peaks. Gaussian fitting was applied to the peaks to accurately determine their centers, facilitating precise measurement of the distance between neutron and gamma peaks. This measurement, with a distance between n/g of 4.1, indicates satisfactory n/γ discrimination performance.

The results illustrate the clear dependence of discrimination performance on operating voltage, underscoring the importance of setting optimal voltages for effective n/γ separation. These findings highlight the value of tuning operating voltages to enhance n/γ discrimination and improve radiation detection accuracy. Future work will focus on further refining these parameters and exploring additional enhancements to detection sensitivity and precision.

References

1. H. R. Bowman, S. G. Thompson, J. C. D. Milton, W. J. Swiatecki, Velocity and angular distributions of prompt neutrons from spontaneous fission of ^{252}Cf , *Physical Review* - 1962. - Vol. 126, No. 6. - P. 2120-2136. <https://doi.org/10.1103/PhysRev.126.2120>
2. C. Budtz-Jorgensen and H.-H. Knitter, Simultaneous investigation of fission fragments and neutrons in $^{252}\text{Cf}(\text{sf})$, *Nuclear Phys A* – 1988. - Vol. 490, P. 307 – 328. [https://doi.org/10.1016/0375-9474\(88\)90508-8](https://doi.org/10.1016/0375-9474(88)90508-8)
3. Shakir Zeynalov, Pavel Sedyshev, Valery Shvetsov and Olga Sidorova, Prompt fission neutron investigation in $^{235}\text{U}(\text{nth},\text{f})$ reaction, *International Conference on Nuclear Data for Science and Technology*, Volume 146, 2017, <https://doi.org/10.1051/epjconf/201714604022>
4. Zeinalov Sh.S., Florek M., Furman W.I., Kriatchkov V.A., Zamyatnin Yu. S., Neutron energy dependence of $^{235}\text{U}(\text{n},\text{f})$ mass and TKE distributions around 8.77 eV resonance VII International Seminar on Interaction of Neutrons with Nuclear – Dubna: JINR, -1999. -E3-1999-212. –P. 258-262.
5. Zeinalov Sh.S., Florek M., Furman W.I., Kriachkov V.A., Zamyatnin Yu.S, Neutron Energy Dependence of Fission Fragment Mass & TKE Distributions of $^{235}\text{U}(\text{n},\text{f})$ - Reaction Below 10 eV, *Dynamical Aspects of Nuclear Fission: Proceedings of the 4-th International Conference - Casta-Papiernicka: Slovak Republic*, - ed. J. Kliman - World Scientific, Singapore, 2000. -P. 417-423.
6. J. Hamsch, H.-H. Knitter, C. Budtz-Jorgensen, and J.P. Theobald, Fission mode fluctuation in the resonances of $^{235}\text{U}(\text{n},\text{f})$, *Nuclear Physics A* -1989. -Vol. 491. –P. 56 – 90.
[https://doi.org/10.1016/0375-9474\(89\)90206-6](https://doi.org/10.1016/0375-9474(89)90206-6)
7. Alf Gook, Franz-Josef Hamsch, and Stephan Oberstedt. *EPJ Web of Conferences* 1 , 05001 (2016)

8. Al-Adili, D. Tarrio, F.-J. Hamsch, A. Gook, K. Jansson, A. Solders, V. Rakopoulos, C. Gustavson, M. Lantz, A. Materrs, S. Oberstedt, A.V. Prokofiev, M. Viladi, M. Osterlund, and S. Pomp, EPJ Web of Conferences 122, 01007 (2016)
9. Joint Institute for Nuclear Research. (n.d.). *ENGREN project*. Retrieved September 5, 2024.
<https://flnp.jinr.int/en-us/main/facilities/materials/engren-project>
10. Eljen Technology. (n.d.). EJ-301, EJ-309 - Neutron/Gamma PSD Liquid Scintillators. Retrieved September 5, 2024, from <https://eljentechnology.com/products/liquid-scintillators/ej-301-ej-309>
11. Scionix. (n.d.). Standard liquid scintillators. Retrieved September 5, 2024, from <https://scionix.nl/standard/#tab-id-3>
12. ET Enterprises. (n.d.). P9821B series photomultipliers. Retrieved September 5, 2024, from <https://et-enterprises.com/products/photomultipliers/product/p9821b-series>
13. Berikov, D. B., Ahmadov, G. S., Kopatch, Y. N., Zhumadilov, K. Sh., & Kuznetsov, V. L. (2019). Digital neutron/gamma discrimination with an organic scintillator. *Recent Contributions to Physics*, 4(71), 29-34. <https://doi.org/10.26577/RCPH-2019-i4-4>
14. Zhang, X., & Su, Y. (2015). Study of digital pulse shape discrimination method. *Chinese Physics C*, 39(1), 29-34. <https://arxiv.org/abs/1502.01807>
15. J. Scherzinger, R. Al Jebali, J.R.M. Annand, K.G. Fissum, R. Hall-Wilton, S. Koufigar, N. Mauritzson, F. Messi, H. Perrey, E. Rofors, A comparison of untagged gamma-ray and tagged-neutron yields from $^{241}\text{AmBe}$ and $^{238}\text{PuBe}$ sources. *Applied Radiation and Isotopes* <https://doi.org/10.1016/j.apradiso.2017.05.014>

16. Akbarov, R. A., Ahmadov, G. S., Ahmadov, F. I., Berikov, D., Holik, M., Mammadov, R., Nuruyev, S. M., Sadigov, A. Z., Sadygov, Z. Y., & Tyutyunnikov, S. I. (2018). Fast neutron detectors with silicon photo-multiplier readouts. *Nuclear Instruments and Methods in Physics Research, A*, 936, 549-551. <https://doi.org/10.1016/j.nima.2018.11.089>